SHAKER CONTROL IN THE PRESENCE OF NONLINEARITIES

Kai Yu[1], Steve Holman[2], and Kelly Brinkley[3]

[1] Department of Electrical Engineering, Stanford University, Stanford, CA 94305 (crazykai@stanford.edu)
[2] Department of Mechanical Engineering, Montana State University, Bozeman, MT 59717 (sbh77@juno.com)
[3] Department of Mechanical Engineering, University of Denver, Denver, CO 80210 (kbrinkle@du.edu)

ABSTRACT

Control systems for shakers are necessary to remove both shaker dynamics as well as coupling effects between the shaker and the structure under test. Little attention has been given to shaker control for nonlinear structures. This paper presents the design, implementation and results of a shaker controller for a horizontal, cantilevered beam subjected to a non-uniform magnetic field. The objective of the shaker control is to ensure the acceleration at the tip of the beam follows a prescribed waveform. The parameters of the nonlinearity were determined using an extended Kalman filter, and the nonlinearity was subsequently cancelled via feedback linearization.

NOMENCLATURE

C	Controller
DOF	Degree(s) of Freedom
EKF	Extended Kalman Filter
P	Plant, or physical system
SISO	Single input, single output

Modal Space

C	System damping matrix
I	Identity matrix
K	System stiffness matrix
M	System mass matrix
MAC	Modal Assurance Critera
POC	Pseudo Orthogonality Criteria
T_U	Mapping matrix between all DOF and reduced DOF
U	Eigenvectors or mode shapes
e	Pertaining to experimentally derived parameters
u	Pertaining to analytically derived parameters
x_n	Entire analytical DOF
x_a	Analytically correlated DOF
x_d	Analytically discarded DOF
Ω^2	Natural frequency of mode shapes
α	Rayleigh damping coefficient for mass weighting
β	Rayleigh damping coefficient for stiffness weighting
ω_n	Homogeneous natural frequency
ζ	Damping ratio

Enhanced Kalman Filter

C	Equivalent strength of magnet ($Nm^{\wedge 3}$)
F	Force from magnet
F_x	Force from magnet in direction tangent to arc of beam
Δ_1	Distance between equilibrium points collinear to F_x

Δ_2 Distance between end of beam and magnet, perpendicular to Δ_1
x Distance towards magnet from initial equilibrium point

Feedback Linearization Controller
B Transfer function relating force applied and acceleration at the end of the beam
B_e Estimated transfer function relating force applied and acceleration at the end of the beam
P_e Estimated plant transfer function
V_l Voltage into the linear plant
V_n Voltage into the nonlinear plant
d Grouped parameter relating magnet force to equivalent magnet strength
$\ddot{x}$ Acceleration of tip of beam

Subscripts

a Analytically reduced matrix (accepted DOF)
n Analytical complete set of DOF

Superscript

FEM Pertaining to the analytical finite element model
G Generalized inverse
T Transpose of a matrix
-1 Inverse

1. INTRODUCTION

Shakers are commonly used in environmental testing and to determine modal parameters of structures. Control systems for shakers are necessary to remove both shaker dynamics as well as coupling effects between the shaker and the structure under test. By inputting a known signal into the shaker and measuring the resulting response, frequency response functions can be developed and modal parameters extracted for modeling. While shaker control systems have been around for decades, little attention has been paid to shaker control in nonlinear systems, even though nonlinear control systems have been evolving over the past two decades[1,2,3]. If nonlinearities in either the structure or environment exist, both the force inputted into the structure and the measured response can by influenced, making it very difficult to extract accurate modal parameters. Therefore, FRF's, while commonly used in nonlinear systems, have to be interpreted differently than if calculated for a linear system.

The purpose of the project is to design and implement a shaker controller that will mitigate the effects of nonlinearity in a structural system. Specifically, it is desired to design a shaker control system that forces the acceleration at the tip of the cantilevered beam to track a 10 Hz sine wave that is input near the fixed end of the beam. The U-magnet placed near the free end of the beam introduces a nonlinear force. The approach to ensuring tracking is fundamentally that of feedback linearization. The nonlinear force exerted on the beam by the magnet is estimated through the use of an extended Kalman filter [4]. Mass, damping, and stiffness matrices used in the Kalman filter are derived using correlation, data reduction, validation, and some linear algebra techniques. The nonlinearity is then cancelled with a feedback linearization controller, and a linear tracking controller is used to ensure the desired tracking is achieved.

The remainder of this paper is organized into the sections of basic control terminology, experimental setup, modal parameter estimation, a discussion of the extended Kalman filter as applied to estimating the parameters of the nonlinearity, design of the feedback linearizing and tracking controllers, experimental results and conclusions.

2. CONTROLS AND CONTROL MODEL DESIGN

In a simple single input, single output (SISO) feedback system, as shown in Figure 2.1, the plant is the system to be controlled [12].

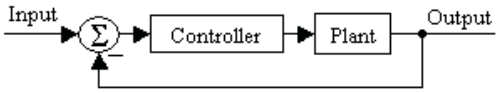

Figure 2.1 - Block Diagram of Simple Feedback System

A controller is designed such that the system transfer function, the ratio of output and input, produces a desired output given an input [12]. Without the feedback loop, the system is "open loop", and the transfer function is [5]:

$$P(s)C(s) \tag{2.1}$$

With the feedback loop, the system is "closed loop", and the transfer function is [12]:

$$\frac{P(s)C(s)}{1+P(s)C(s)} \tag{2.2}$$

In an open loop system the controller has no information of how it has influenced the output, while in a closed loop system the controller uses the measured output to control the system. While numerous controller designs exist, many are only applicable with plants that behave linearly. However, some designs have proven effective in non-linear systems, most notably Lyapanov methods [13], adaptive and predictive controls [14], and the extended Kalman filter.

3. EXPERIMENTAL DESCRIPTION

The test structure is shown in figure 3.1 and consists of a 6061-aluminum alloy cantilevered beam of dimensions 24 x 2 x .125 inches (61 x 5.1 x .32 cm). A steel piece of dimensions 1 x 2 x .125 inches (2.5 x 5.1 x .32 cm) was attached by screws to the free end of the beam. Five inches (12.7 cm) from the fixed end of the beam, a stinger was threaded through the beam and connected to a Labworks ET-132-2 shaker. The stinger attachment was not ideal in the sense that it produced undesired torsional moments and axial reactions. This effect was absorbed into the "plant" and so became a moot point. The non-ideal stinger did provide some complications later when an analytical model was developed. Nonlinearity was introduced by placing a U-magnet of dimensions 1 x 1 x 1.44 inches (2.5 x 2.5 x 3.66 cm) and a characteristic gap of .38 inches (.97 cm) at the free end of the cantilever beam. The bottom of the magnet was aligned with the bottom of the beam and placed .41 inches (1.0 cm) from the beam. This placement allowed the beam to move freely without touching the magnet, ensuring no contact nonlinearities would be introduced. The attraction of the steel piece and the magnet created a second equilibrium point for the beam .45 inches (1.1 cm) away from its natural equilibrium point.

To determine the modal parameters of the beam from the impact tests, a four-channel Dactron Photon data acquisition system was utilized. When the shaker was not attached, a PCB 086C03 impact hammer with a soft plastic tip was used to excite the structure. The soft plastic tip was chosen so that it would predominantly excite the first three bending modes. When the shaker was attached, a sine chirp ranging from 1-250 Hz in ten seconds was input into the shaker. Three PCB 352A24 accelerometers were placed equidistantly along the midplane of the beam. These measurements were obtained using the DACTRON Photon FFT Analyzer and the FRF data was reduced using the Vibrant Technology ME'scope software.

The data acquisition system for the control experiments was composed of a PC running the Mathworks XPC Target real time operating system. The PC was equipped with a National Instruments PCI-6052E data acquisition board. Output signals were amplified by a Labworks PA-138 amplifier and sent to the shaker. A PCB 352A24 teardrop-style accelerometer was attached to the free end of the cantilever beam to measure acceleration. Software required to run the data acquisition system included MATLAB, Simulink, the Real-Time Workshop, and a C compiler. For each test run, the controller created in Simulink was built and sent to the signal conditioner via the network by xPC Target.

To illustrate the picture below, the letters correspond to the following equipment (PC not shown):

a. National Instruments signal conditioner SC2345
b. Labworks PA-138 amplifier

c. Labworks ET-132-2 electromechanical shaker
d. Test Structure – 6061 Aluminum
e. Permanent, stationary U-magnet

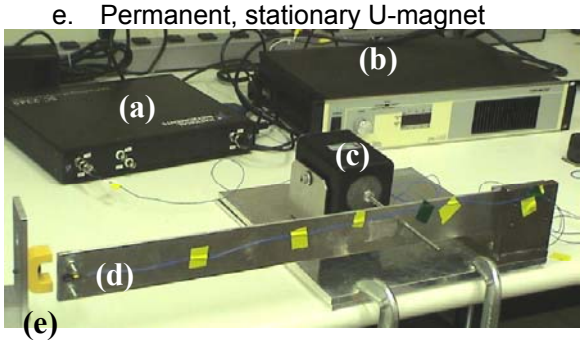

4. MODAL PARAMETER ESTIMATION

In the course of developing a model-based control algorithm, estimation of the system mass [M], damping [C], and stiffness [K] matrices was required. The complete plant consisted of the mechanical structure as well as the electromechanical dynamics from the shaker and unknown dynamics from the signal conditioner and amplifier. It is therefore potentially difficult to obtain an accurate set of system matrices. Initially, to help alleviate this problem the shaker was disconnected and only the beam was considered.

The first step was to perform an impact hammer test on the structure to obtain modal data. Next, a finite element model was developed to give predicted modal data [5,8].

It was then necessary to quantitatively compare the two data sets. A data reduction scheme known as system equivalent reduction expansion process (SEREP) was employed on the analytical model data [7,8,11]. This process formed a mapping between the total number of analytical degrees of freedom (DOF) and the experimental degrees of freedom. Through this method, a well-correlated and truncated set of degrees of freedom was produced and still retained the original fidelity of the analytical model.

The following equation illustrates the relationship between the accepted, or retained, degrees of freedom and the discarded degrees of freedom

$$\{x_n\}=\begin{Bmatrix} x_a \\ x_d \end{Bmatrix}=[T]\{x_a\} \tag{4.1}$$

where x_a is the accepted set of degrees of freedom and x_d is the discarded degrees of freedom. The reduced matrices can be determined from

$$\begin{aligned} [M_a]&=[T_U]^T[M_n][T_U] \\ [K_a]&=[T_U]^T[K_n][T_U] \end{aligned} \tag{4.2}$$

where

$$[\mathrm{T_U}]=[\mathrm{U_n}][\mathrm{U_a}]^{\mathrm{g}} \tag{4.3}$$

and U_n is the modal shape vector for all degrees of freedom and U_a is the modal shape vector for only the accepted degrees of freedom.

Then, in order to validate that this procedure represents the actual system, inclusive of the shaker and electronics, comparisons were made with respect to the eigenvectors produced by the experimental and analytical models. The mode shapes were compared using the Modal Assurance Criteria (MAC) [6,8]

$$\mathrm{MAC_{ij}}=\frac{\left[\{\mathrm{u_i}\}^{\mathrm{T}}\{\mathrm{e_j}\}\right]^2}{\left[\{\mathrm{u_i}\}^{\mathrm{T}}\{\mathrm{u_i}\}\right]\left[\{\mathrm{e_j}\}^{\mathrm{T}}\{\mathrm{e_j}\}\right]} \tag{4.4}$$

where u_i and e_i are the analytical and experimental modal shape vectors, respectively.
and the Pseudo Orthogonality Check (POC) [7,8].

$$POC = [E]^T [M][U] \stackrel{?}{=} [I] \tag{4.5}$$

The results of these checks are shown in Figures 7.1-1 and 7.1-2, respectively.

Next, an estimate of the reduced mass and stiffness system matrices were determined using two approaches. The first method incorporated the SEREP method outlined above for the analytical model. The second method used the generalized inverse of the modal vectors for the system using

$$\begin{aligned} \left[\mathrm{U}^{\mathrm{g}}\right]^{\mathrm{T}}[\mathrm{I}]\left[\mathrm{U}^{\mathrm{g}}\right] &= \left[\mathrm{M}^{\mathrm{FEM}}\right] \\ \left[\mathrm{U}^{\mathrm{g}}\right]^{\mathrm{T}}\left[\Omega^2\right]\left[\mathrm{U}^{\mathrm{g}}\right] &= \left[\mathrm{K}^{\mathrm{FEM}}\right] \\ \left[U^{g}\right]^{T}\left[\overline{2\zeta\omega_n}\right]\left[U^{g}\right] &= \left[C^{FEM}\right] \end{aligned} \tag{4.6}$$

where $\left[\mathrm{U}\right]^{\mathrm{g}} = \left[\left[\mathrm{U}\right]^{\mathrm{T}}\left[\mathrm{U}\right]\right]^{-1}\left[\mathrm{U}\right]^{\mathrm{T}}$ or $\left[\mathrm{U}\right]^{\mathrm{g}} = \left[\mathrm{U}\right]^{-1}$ (4.7)

for a square matrix. The damping matrix was developed using a proportional approximation. This method is called Rayleigh damping, whereby the damping matrix is related to the linear combinations of the mass and stiffness matrices.

$$[C] = \alpha[M] + \beta[K] \tag{4.8}$$

Here alpha and beta are the Rayleigh damping coefficients and relate to each other by

$$\frac{\alpha + \beta\omega^2}{2\omega} = \zeta \tag{4.9}$$

Rayleigh damping uncouples every mode from every other mode. The modes are therefore linearly independent. The generalized inverse takes the modal damping in modal space and projects it to physical space to obtain the estimate for the physical damping matrix. MEscope's curve fitting process is also based on proportional damping, which is why the matrix is diagonal in modal space [9]. Natural frequencies and modal damping are obtained from MEscope and therefore facilitates the software to make an accurate physical damping matrix.

Both of these approaches estimated the exact same analytical mass and stiffness matrices. This same process was extended to encompass the measured experimental shape vectors using

$$\begin{aligned} \left[\mathrm{E}^{\mathrm{g}}\right]^{\mathrm{T}}[\mathrm{I}]\left[\mathrm{E}^{\mathrm{g}}\right] &= [\mathrm{M}] \\ \left[\mathrm{E}^{\mathrm{g}}\right]^{\mathrm{T}}\left[\Omega^2\right]\left[\mathrm{E}^{\mathrm{g}}\right] &= [\mathrm{K}] \end{aligned} \tag{4.10}$$

where

$$\left[\mathrm{E}\right]^{\mathrm{g}} = \left[\left[\mathrm{E}\right]^{\mathrm{T}}\left[\mathrm{E}\right]\right]^{-1}\left[\mathrm{E}\right]^{\mathrm{T}} \quad \text{or} \quad \left[\mathrm{E}\right]^{\mathrm{g}} = \left[\mathrm{E}\right]^{-1} \text{ for a square matrix.} \tag{4.11}$$

Once the measured experimental mass and stiffness system matrices were developed, they were compared to the system matrices that were analytically derived. The results of this comparison showed that the system matrices were in close agreement. These results validated this process to be used on the actual plant, inclusive of the shaker and electronics.

Lastly, the experimental frequency response functions of the real plant were obtained through the DACTRON Photon FFT analyzer and the modal parameters were extracted using the MEscope Modal Analysis software. The system matrices were then computed using the same procedures outlined above.

5. EXTENDED KALMAN FILTER IMPLEMENTATION

As a state estimator, the extended Kalman filter (EKF) utilizes a predictor/corrector technique to estimate states governed by a time varying process [4]. Unlike an ordinary Kalman filter, the extended Kalman filter first linearizes the estimation with respect to the mean and the covariance of the current state and then independently solves for each point in time. Two sets of equations characterize the filter: 1) time update equations that function

as the predictor and 2) measurement update equations, which function as the corrector. The former projects the current state along with error covariance into the next time step while the latter incorporates new measurements that are adjusted by the Kalman gain into the predictor estimate. Using a three-degree of freedom model to describe the system being estimated, the EKF is validated when constant parameters are estimated and converge to the given initial conditions.

In this application, the extended Kalman filter was used to estimate unknown attributes of the magnetic force, namely, the strength of the magnet and distances from the free end of the beam. The magnetic force was assumed to be [15]:

$$F = \frac{C}{d^3} \qquad (5.1)$$Only the lateral component of the force was of interest and is given by

$$F_x = \frac{C(\Delta_1 - x)}{[(\Delta_1 - x)^2 + \Delta_2^2]^2} \qquad (5.2)$$

where Δ_1, Δ_2 and C are distances from the tip of the beam to the magnet and the strength of the magnet, respectively (Figure 5.1). Assuming a three-degree of freedom model with viscous damping to represent the beam, equations of motion were developed, which used the calculated mass, stiffness, and damping matrices. A Matlab[10] model was developed using simulated displacement data to verify that *C*, Δ_1, and Δ_2 estimates converged. Once the script was verified, it was adjusted to incorporate experimental displacement data. Acceleration time histories from the three modeled points were collected, integrated twice, and high-pass filtered to produce displacement. The Matlab "cumtrapz" was used to integrate the data. The Matlab "filtfilt" command was used to high-pass filter the data in both directions, eliminating the low-frequency trends without introducing phase error. Using this displacement data, the strength and distance parameters were determined and checked for convergence.

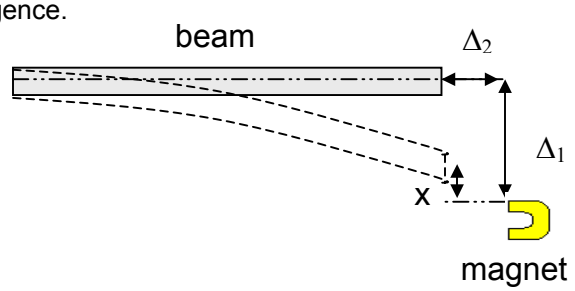

Figure 5.1 - Assumed geometry for distance and displacement at the end of the beam

6. CONTROL DESIGN

Two controllers, a tracking controller and a feedback linearization controller, were designed.

6.1 Tracking Controller

A tracking controller seeks to force the output waveform to be equal to the input waveform. By setting the gain of the open loop transfer function (equation 2.1) at a particular frequency, the gain and phase of the closed loop transfer function (equation 2.2) at that frequency are equal to one and zero, respectively. Any input at that particular frequency will then be outputted with the same amplitude and phase. For this project a tracking controller that tracks a 10 Hz sinusoid of amplitude 0.5V was designed.

6.2 Feedback Linearization Controller

The block diagram in Figure 6.2 depicts the system when the magnet is not attached. The equation for the acceleration was written as:

$$\ddot{x} = PV_l \qquad (6.1)$$

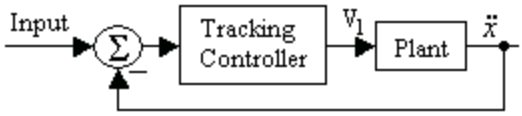

Figure 6.2 – Block diagram of system without magnet

With the magnet added, the acceleration was:

$$\ddot{x} = PV_n + BF_m(x) \tag{6.2}$$

The effect of the magnet was subtracted out by setting:

$$V_n = V_l - P_e^{-1} B_e F_x(x) \tag{6.3}$$

where F_x was estimated by equation 5.2, and the parameters of this equation were estimated by the Kalman filter discussed in the previous section. To determine displacement the acceleration was integrated twice and high-pass filtered to remove any DC offset and other low-frequency trends in the acceleration. P_e and B_e were easily estimated by developing a transfer function whose frequency response closely matched the frequency response function of the tip of the beam and plant, respectively.

The new plant became the combination of the plant without the magnet, the effect of the magnet, and the feedback linearization controller. In theory, if F_x estimates the effect of the magnet well, it will eliminate the effect of the magnet and the tracking controller should track with no steady state error. A block diagram of the system with the magnet is below.

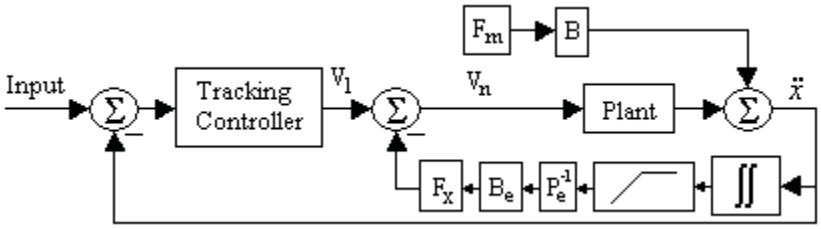

Figure 6.3 – Block diagram of system with magnet

7. RESULTS

Without the magnet attached, the tracking controller was able to track a 0.5V amplitude sinusoid at 10 Hz, as seen in Figure 7.1.

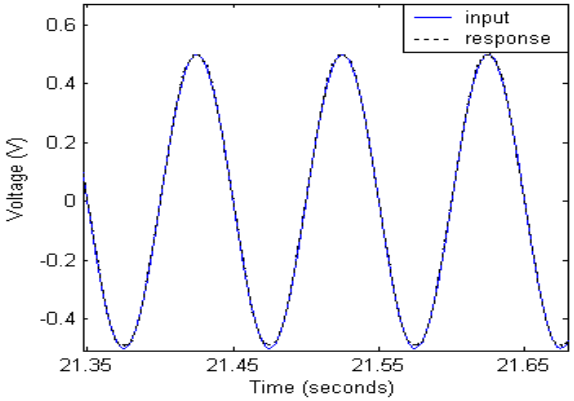

Figure 7.1 – Response measured of a 0.5V sine wave input at 10 Hz with no magnet attached

With the introduction of the magnet, at low input amplitudes the controller designed to track 10 Hz was still able to maintain the phase and overall shape of the sine wave. However, the response exhibited bleeding, where the

peaks and troughs were lower than the inputted wave. At input amplitudes of at least .5V, the beam came close enough to the magnet to be pulled into a remote, non-periodic attractor.

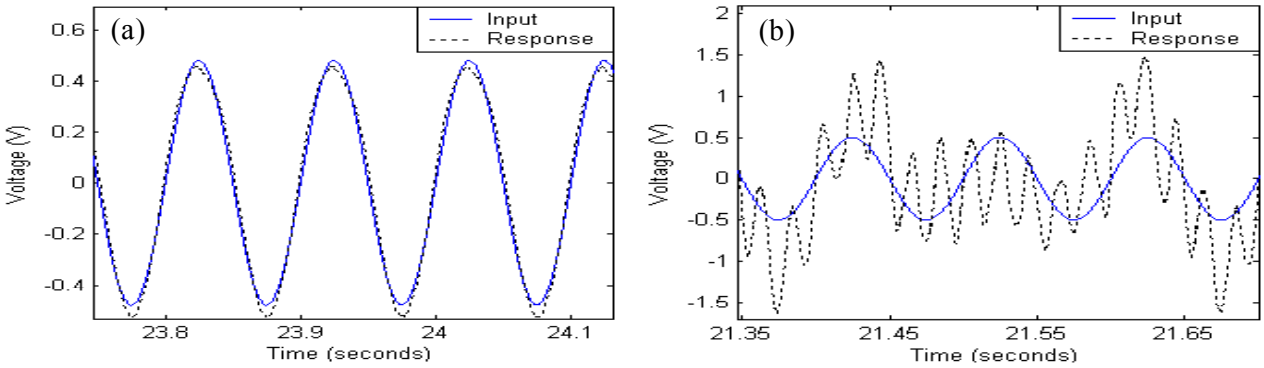

Figure 7.2 - Response measured with the magnet attached of a 10 Hz sine wave input with an amplitude of (a) 0.48 V (b) 0.5 V

7.1 Modal Parameter Estimation Results

The MAC and POC values are in Tables 7.1-1 and 7.1-2, respectively. The MAC is an expedient method for obtaining a first indication of how well the analytical and experimental vectors correlate. As can be seen by the tabled results, the diagonal matrix contained values that were all close to one. This then indicated a high level of correlation. MAC(2,3), indicating mode 2 from the analytical model and mode 3 from the experimental results, showed a significant amount of correlation with respect to the other off diagonal terms. However, in light of the fact that the diagonal terms were so close to one, it was assumed that the modal vectors were well correlated.

Table 7.1-1 - Modal Assurance Criteria with Stinger		
0.9947	0.0550	0.0624
0.0314	**0.9963**	0.2253
0.0785	0.0752	**0.9664**

Table 7.1-2 - Pseudo Orthogonality Check with Stinger		
0.9977	-0.0625	0.0243
-0.0059	**-0.9978**	-0.0664
-0.1004	0.1810	**-0.9783**

Pertaining to the POC, this formulation is simply a comparison between the analytical modal vector and the experimental modal vector. To be able to employ this triple product, all matrices must have equal inner dimensions. For this to occur, a necessary data expansion or reduction, or both, was necessary. To achieve matrices with equal inner dimensions a finite element model was constructed with many DOFs and then truncated down to the high fidelity model. In regards to the negative values in the diagonal, even though the modal displacement vectors have negative quantities here (due to the shape of the 2nd and 3rd bending modes), the reason that they are negative was simply that the sum of the three products for each term in the matrix was negative because of the relative magnitudes.

7.2 Extended Kalman Filter Estimation Results

For the simulated EKF, estimated values of C, Δ_1, and Δ_2 converged to given parameters which verified the model. Sensitivity of the model was also examined. Although amplitude of the forcing function made less than 1% difference in the convergence, initial conditions and estimates were highly sensitive parameters. Convergence only occurred on 10^{-2} m and 10^{-3} m orders of magnitude as long as the estimate was within ±50% of the initial condition. Experimental data in the filter showed that C oscillated in the range of ±1e-5 Nm^3 rather than converging, thus indicating the force of the magnet was more complex than modeled. Values of Δ_1 and Δ_2 did not converge either, however, they were well behaved and stayed within one order of magnitude. Although convergence did not occur for these parameters, only the order of magnitude was required to make an initial design for a controller. Through the estimation of these parameters, the nonlinear effect of the magnet was determined and subtracted from the input to the shaker.

To verify that C, Δ_1, and Δ_2 were reasonably estimated, the equilibrium points of the beam were found by substituting the force from the magnet into the static deflection equation. Since C oscillated, the average value of 1.05e-7 Nm^3 was input; however, an equilibrium point at 0.008m was found that was not physically represented in the system. By slightly adjusting C to 1e-8 Nm^3, which is within one standard deviation (1.1e-6 $Nm^{3)}$, three equilibrium points were found at 0.00016m, 0.0058m, and 0.0080m. The first and third points were visually confirmed although the second was not because it is unstable. The need to adjust C further confirmed that the model approximated, but did not completely describe the system.

7.3 Structure with Feedback Linearization Controller

The estimates from the extended Kalman filter provided good estimates for the parameters Δ_1, Δ_2. However, for the feedback linearization controller to compensate for the nonlinearities, the Δ_1 and Δ_2 were adjusted to .006 cm and .001 cm respectively. The adjustment was probably needed because the equation 5.2, which modeled the lateral component of the magnetic force, did not characterize the magnetic force correctly.

With the feedback linearization controller the system could now track at .5V in the presence of the magnet. The controller was able to track amplitudes up to .52V. At higher amplitudes more gain was needed to counteract the effects of the magnet, but the D/A channel saturated at 10 V, so with the equipment available we were not able to achieve stability. At amplitudes lower than .5V the feedback linearization controller had negligible effect and did not adversely affect the stability of the system.

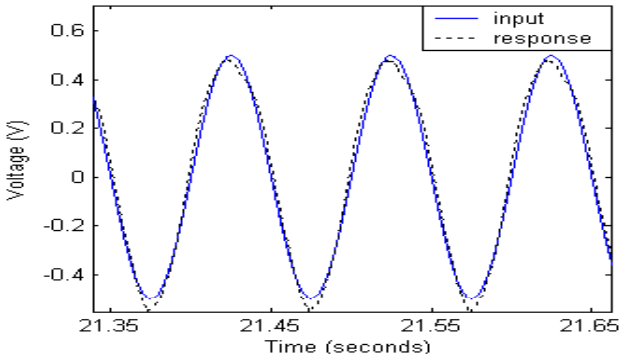

Figure 7.3 - Sample of response measured of a 10 Hz sine wave input with an amplitude of .5V with controller

8. CONCLUSION

Using an extended Kalman filter proved effective in estimating the parameters that determine nonlinearity, and the feedback linearization controller used those values to make the unstable system stable. Although the feedback linearization controller did not eliminate the force of the magnet, it compensated for the nonlinearity enough to allow tracking at higher amplitudes. While the parameters could have been measured by hand, had the nonlinearity been inaccessible the extended Kalman filter would have still been able to estimate the parameters. This project demonstrated that in a simple structure with a well-defined nonlinearity, shaker control can be developed to mitigate the effect of the nonlinearity.

Recommendations for future research include the following:

1. Apply the same technique on a more complex structure
2. Apply the same technique with a less well-defined nonlinearity
3. Create a tracking controller over a broader frequency range and test the tracking

9. ACKNOWLEDGEMENTS

We would like to extend our thanks and appreciation to our mentor Dr. Matt Bement for his guidance and assistance in the development of all aspects of this project and to Dr. Peter Avitabile for his guidance in using data reduction schemes, correlation, system matrix estimation, and help with countless software packages. Furthermore, we would like to thank Dr. Charles R. Farrar for coordinating the Los Alamos Dynamics Summer School program. This work was supported by the Department of Energy's Education Programs Office and the

Engineering Science and Applications Division at Los Alamos National Laboratory.. We would also like to thank the following companies for providing the software and hardware for this project:
Vibrant Technologies (MEscope experimental modal analysis software),
The Mathworks, Inc. (numerical analysis software including xpcTarget and Simulink),
Dynamic Design Solutions n.v. (DDS) (FEMtools Theoretical v. 1.4),
and Hibbitt, Karlsson, and Sorensen, Inc. (ABAQUS finite element software).

10. REFERENCES

[1] Isidori, Alberto. Nonlinear Control Systems (3rd edition), Springer Verlag (1995),

[2] Elliott, D.L., "Book Reviews", International Journal of Robust and Nonlinear Control, 2003; 13:91-93

[3] Yu, Jie; Jadbabaie, Ali; Primbs, James; and Huang, Yun. "Comparison of Nonlinear Control Designs for a Ducted Fan Model", International Federation of Automatic Control, 1999

[4] Welsch, Greg and Bishop, Gary. "An Introduction to the Kalman Filter", Department of Computer Science University of North Carolina at Chapel Hill, Chapel Hill, NC 27599-3175

[5] Avitabile, P. and O'Callahan, J.C., Matlab scripts for FEA. October, 1994

[6] Allemang, R.J. and Brown, D.L., "A Correlation Coefficient for Modal Vector Analysis", First International Modal Analysis Conference, Orlando, Florida, November 1982, pp. 110-116

[7] Avitabile, P., O'Callahan, J.C., and Milani, J., "Model Correlation and Orthogonality Criteria", Sixth International Modal Analysis Conference, Orlando, Florida, February 1988, pp. 1039-1047

[8] Personal communication with Peter Avitabile.

[9] MEscope. Vibrant Technologies, Inc.

[10] MATLAB toolbox – Simulink, The MathWorks

[11] O'Callahan, J.C., Avitabile, P., and Riemer, R., "System Equivalent Reduction Expansion Process", Seventh International Modal Analysis Conference, Las Vegas, Nevada, February 1989, pp. 29-37

[12] Franklin, Gene F., Powell, J. David, and Emami-Naeini, Abbas, Feedback Control of Dynamic Systems, Addison-Wesley Publishing Company, Third Edition, 1994

[13] Hammami, M. A., "On the Stability of Nonlinear Control Systems with Uncertainty", Journal of Dynamical and Control Systems; April 2001; V. 7. no. 2, p. 171-179

[14] Tan, K. K., Lee, T. H., Huang, S. N., Leu, F. M., "Adaptive-Predictive Control of a Class of SISO Nonlinear Systems", Dynamics and Control; April 2001; v. 11, no. 2, p. 151-174

[15] Serway, Raymond A., Physics for Scientists and Engineers, Saunders College Publishing, Third Edition, 1990